TALLINN UNIVERSITY OF TECHNOLOGY
School of Information Technologies

Andrei Krotov 178186IVEM

DYNAMICAL SIMULATION OF AORTIC-RADIAL BLOODFLOW

Master's thesis

Supervisor: Paul Annus
PhD
Co-supervisor: Hip Kõiv
MSc
Rauno Jõemaa
MSc

Tallinn 2019

TALLINNA TEHNIKAÜLIKOOL
Infotehnoloogia teaduskond

Andrei Krotov 178186IVEM

DÜNAAMILINE VERE VOOLU SIMULATSIOON AORDIST RADIAALARTERINI

Magistritöö

Juhendaja: Paul Annus
Doktorikraad
Kaasjuhendaja Hip Kõiv
Magistrikraad
Rauno Jõemaa
Magistrikraad

Tallinn 2019

Author’s declaration of originality

I hereby certify that I am the sole author of this thesis. All the used materials, references to the literature and the work of others have been referred to. This thesis has not been presented for examination anywhere else.

Author: Andrei Krotov

06.05.2019

Abstract

This thesis is the final educational task to get the Master of Science degree at the Tallinn University of Technology.

Aim of this thesis was to simulate pulsating blood flow through composed aortic-radial blood transition path model and provide experiments to investigate suitability of biomedical measurements for cardiovascular system analysis. This thesis consists of two parts: theoretical background overview and practical experiments with explanations. First part has an overview of timely state-of-the-art in simulation-based experiments for cardiovascular system analysis, anatomical background of blood supply system and bioimpedance measurement. First part of the work was mainly composed by analysing literature and combining known facts. Second part has complete descriptions of provided experiments, starting from model drawing and ending with results evaluation and discussion. Based on gathered dimensional and physical parameters from the literature 3D CAD model of aortic to radial blood path was drawn. Using different simulation modules and physics together with four electrode bioimpedance sensing technique setups the simulation was set up. First experiments analysed changes in blood internal structure that can reflect on bioimpedance measurement. After moved on to experiments that analysed the impedance change relation to pulsating blood flow and dimensional changes in the blood vessels caused by CVD's.

The simulation met the wanted requirements for this thesis. Changes in bioimpedance measurement result are related to blood consistency and blood vessel dimensional changes. None of the changes are linear and are complex across the whole cardiovascular system. The results of the simulation were consistent to theoretical overview in the first part of the thesis. Thesis consists of practically usable results and facts for possible evolvement of current topic.

This thesis is written in English and is 56 pages long, including 9 chapters, 25 figures and 5 tables.

Annotatsioon

DÜNAAMILINE VERE VOOLU SIMULATSIOON AORDIST RADIAALARTERINI

Antud magistritöö on viimaseks õppekavas ettenähtud ülesandeks, mida on vaja täita Magistrikraadi omandamiseks Tallinna Tehnikaülikoolist.

Antud töö põhieesmärgiks oli pulseeriva vere voolu simuleerimine vereringe osas aordist radiaalarterini ja biomeditsiinilise mõõtmise rakendamine sellel, et välja selgitada kas antud meetod on sobilik vereringesüsteemi analüüsiks. Töö koosneb kahest osast: teoreetiline osa, kus on kirjeldatud anatoomilt ja füüsikalist tausta, ning praktilisest osas, mis sisaldab endast põhjalikku ülevaadet läbiviidud katsetest ning tulemustest. Esimeses osas on välja toodud hetkeline teadustase uuringutes ja teadmistes millele sarnaneb või toetub antud töö. Kirjanduse kokku kogumisel ning analüüsil sai koostatud baasteadmiste kogum, milles sisaldub anatoomiline taust inimese vereringesüsteemist, bioimpedantsi mõõtmise põhiteadmised ning füüsikalised selgitused ning parameetrid dünaamilise simulatsiooni ülesseadmiseks. Teises osas on kirjeldatud katsete läbiviimist alustades mudeli koostamisest kuni tulemuste esitlemiseni ja arutlemiseni. Praktilises osas uuriti esmalt vere struktuursete muutuste väljapaistmist impedantsi mõõtetulemustes, milleks olid vere koostise uuring ja olemasolevate teooriate väljatoomine. Seejärel viidi läbi katseid dimensionaalsete muutustega veresoone seinas, mis olid põhjustatud pulseeriva vere voolu poolt. Muutuste all vaadeldi eraldi füsioloogilisi muutusi, mis olid tingitud südame pulseerivatest impulssidest ning enamlevinud vereringe kahjustustest ja haigustest. Selleks olid muutused jaotatud pika- ning lühiajalisteks muutusteks. Bioimpedantsi mõõdeti kasutades nelja elektroodiga mõõtemeetodit. Simulatsioon oli läbi viidud ideaalsetes tingimustes ning tehtud nii mitmeid lihtsustusi. Lihtsustustest võib välja tuua puudusi vereliiklus teekonnas aordist radiaalarterini, kus on sirgjoonelised rajad ning väga vähesed paindumised, veresooned on jäigad ning nende positsioon ruumis ei muutu välja arvatud nende läbimõõt.

Tulemustest tulenes, et igasugused muutused vereringesüsteemis kajastuvad bioimpedantsi mõõtetulemustest. Kuna kogu vereringesüsteem on väga keeruline siis puuduvad ka siinkohal lineaarsed seosed. Tulemustest saab välja tuua põhilised milleks on võimalus uurida vere koostist impedantsi abil, impedantsi mõõtetulemuse graafikutes kajastuvad vere voolu pulsatsioonid ning veresoonkonna haigustest tingitud defektid. Antud tööga kinnitatakse võimalust kasutada bioimpedantsi vereringe süsteemi analüüsimiseks. Töös välja toodud teadmisi ning tulemusi on sobilik kasutada antud teema arendamiseks, tehes mudelit realistlikumaks ning lisades simulatsioonile detaile.

Lõputöö on kirjutatud inglise keeles ning sisaldab teksti 56 leheküljel, 9 peatükki, 25 joonist, 5 tabelit.

List of abbreviations and terms

pH	Measure of acidity
WSS	Wall shear stress
IT	Info technology
CAD	Computer-aided design
1D	One-dimensional space
2D	Two-dimensional space
3D	Three-dimensional space
FEM	Finite element method
PDE	Partial differential equation
CVD	Cardiovascular disease
CAP	Central aortic pressure
Pa	Pascal (SI pressure unit)
mmHg	Millimetre of mercury (pressure unit)
AC	Alternating current
DC	Direct current
CAE	Computer-aided engineering
PTT	Pulse transit time
SF-BIA	Single frequency bioelectrical impedance analysis

Table of contents

List of figures

List of tables

1 Introduction

The cardiovascular system is an organ system that has many functions to serve the needs of a human organism. The main function is to transport the blood together with oxygen, nutrients, hormones and other gases between the cells of different organs. In addition to transportation function it takes part of body temperature and pH regulation [1]. Blood carries the needed substances to maintain stable functionality of all body organs and plays a significant role to help the body fight against diseases. Because of the high importance of the cardiovascular system, it has been a popular investigation field of human body through many years.

To study cardiovascular system healthiness individual measurements for every patient should be carried out. New possibilities in biomedicine have growing tendency of providing non-invasive diagnostics using bioimpedance analysis. Different structural and motion caused changes in cardiovascular system affect electrical properties of blood. Using four electrode sensing setup the electric current conducting properties of the blood can be studied by measuring impedance. By using this diagnostics method it should be possible to detect changes in the cardiovascular system caused by pulsating blood flow, diseases and change in blood consistency. These theoretical claims would be tested experimentally within this thesis using simulation-based approach.

This thesis consists of two parts, first part is an overview of state-of-the-art, anatomical and physical background, the second part is about practical use of knowledge gathered together in the first part. Practical part is about making a simplified aortic to radial blood path model and providing dynamic blood flow and bioimpedance measurement simulation. Evaluated results are used to get as much as possible from the potential of composed simulation. Cardiovascular system describing parameters like wall shear stress (WSS), pressure waveforms, velocity waveforms, impedance to volume relation and other flow related parameters are under interest. The results are going to be analysed and discussed in perspective of theoretical background overviewed in the first part.

Previous studies are related to specific studies of cardiovascular system using simulation of pulsating blood flow for analysing disease prevention, detection and treatment possibilities. These simulations have geometries of different parts of cardiovascular system where the disease formation can take place. Study done in this thesis is unique and useful because it studies the whole aortal to radial blood transition path using bioimpedance analysis method. Provided experiments are intended to show practical usage of impedance sensing to detect different changes in cardiovascular system caused by physiological factors or diseases.

Main goals of the study are:

1. Overview current state-of-the-art, anatomy and physics behind human cardiovascular system, bioimpedance theory and measurement technique;

2. Compose aortic to radial blood path model;

3. Simulate pulsating blood flow and different disease caused defects that can affect bioimpedance measurement;

4. Evaluate bioimpedance measurement results to estimate suitability for detecting different changes in cardiovascular system.

2 State-of-the-art overview

Some of the timely articles which have similar methodology or study interest are reviewed in current chapter in addition to those which were used for comparison and realisation of the up-to-date state of the art. In addition, the articles and investigations of previously published paperwork's that the setup of simulation is based on are reviewed together with brief introduction to cardiovascular system anatomy and bioimpedance measurement.

2.1 Simulation based study

Simulation-based studies become more popular with the evolvement of IT technologies and computer-aided design (CAD) modelling possibilities. Simulation allows user to test something without physically making it and not affecting actual environment, at the same time getting a very good visualization of the system. The simulation is enclosed environment and gives direct outcomes for the input defined by the user. It would not have any disturbances from influencers outside of the system and will be simulated in so called ideal conditions. Results will be same if the input is not changed and does not have any dependence to repeat count. System automatically adapts itself to the change of every parameter [2]. Current thesis practical part was simulation based because a lot of experiments with lots of variable changes had to be performed which would be time consuming and materially costly. Due to the practical part with lots of experiments simulation allows to make mistakes in decisions without any losses besides the computational time.

Researchers use computational modeling techniques to simulate cardiovascular system behaviour and design the devices for disease treatment or diagnosis like artificial heart valves, pacemakers or non-invasive medical diagnostic equipment. In this case computers are used to simulate and study the behaviour of complex systems. Simulated systems have mathematical and physical input parameters and as a result the output is computed. Outcomes are observed and analysed by changing or adjusting different variables alone

or in combination [3]. This way simulation operator should only be aware of correct input and requested output, leaving the computational part to be done by the computer.

Used simulation cross-platform is based on finite element method (FEM) analysis. FEM was introduced in 1940's when Henrikoff and Courant developed a system for elasticity and structural analysis in civil and aeronautical engineering [4]. FEM is used to analyse different physical phenomenon's using numerical technique. Physical properties like fluid flow, thermal distribution, pulse and wave propagation, current flow and others are described by partial differential equations (PDE's). For solving PDE's most prominent technique today is FEM based. FEM itself is based on principle of energy minimization. When force or some any other boundary condition is applied to a body it has many possible change solutions and modifications but only one should be chosen as correct. Minimization of energy principle chooses the solution where the total energy is lowest [5].

COMSOL is the software we have today that is capable to provide analysis for over 30 different research fields. COMSOL Multiphysics versions 5.2 and 5.4 were used for simulation of aortic to radial blood flow simulation. This software allows us to draw simple geometric designs in 1D, 2D and 3D. Define material properties to drawn or imported geometries also adding the physical properties. After all the definitions and parametric variables are given to the geometry the study type can be chosen static or time dependent, and different results and measurements evaluated and visualized.

One of the simulation inputs is the geometry that the simulation will be provided on. Model was suggested to be made in 3D which would be more realistic and have more detailed visualizing possibilities. To draw the 3D model for simulation the CAD software was used. The numerical control system which later was called CAD was founded by Dr. Patrick Hanratty in 1957 and in this work the Autodesk AutoCAD 2017 software was used for drawing [6].

2.2 Aortic disease diagnosis through measurement form radial artery

Cardiovascular diseases (CVD's) are disorders related to heart and blood vessels. 1.1 billion of whole world population adults have high blood pressure known as hypertension and only one out of five has it under control. 17.9 million people die yearly from CVD's,

which makes them the most frequent cause of death [7]. Blood pressure reflects functionality of cardiovascular system and has direct influence from different diseases. Therefore, measuring and keeping the blood pressure under control is important.

Most known CVD's are atherosclerosis and endothelian dysfunction, both clogging or entirely blocking blood vessels. First is related to plaque growth on arterial walls and the second is dysfunction of endothelium which keeps the plaque away and makes arteries elastic. Other diseases are also somehow related to poor blood flow mainly because the heart is not pushing enough blood through cardiovascular system, caused by heart muscle malfunction, heart valve leak or disorder. Or the bad flow properties of arteries if they are clogged, blocked or nonelastic [8].

CVD's are directly related to central aortic pressure (CAP) [9]. The sphygmomanometer that measures the arterial blood pressure from brachial artery has been around for over 100 years. CAP is suggested to be more related to future cardiovascular events and has different behaviour than pressure measured from brachial artery. Over the years it was proven that arterial pressure measured from the brachial artery is a poor surrogate for aortic pressure estimation which is significantly lower [10]. The diastolic pressure does not differ much across large arteries, but the systolic pressure may have difference of 11-13 mmHg [11].

Many studies [10], [12], [13] suggest measuring CAP from radial artery is more informative non-invasive way to get blood flow parameter readings. With adaptive transfer functions CAP can be evaluated from radial pressure waveform measured using tonometer in pair with sphygmomanometer or some other non-invasive way to retrieve blood pressure waveform. The radial artery is preferred because the pulse on forearm from radial artery is readily felt and artery movement is limited. Brachial and carotid arteries are mobile and hard to be fixated for measurement [10], [12]. Current study estimates that bioimpedance will be used to measure blood pressure waveform from radial artery.

2.3 Previous usage of similar simulation-based studies

Authors previous study was based on bioimpedance measurement from the forearm with evaluation of measurement sensitivity areas with different placement of electrodes and

studying current density waves propagation in tissues. Bioimpedance measurement was proven possible from radial artery on a static model [14]. In this study the dynamic model will be made including blood flow and not only forearm under investigation but whole aortic to radial blood transition path. Using previous knowledge of electrical impedance related simulations in this work bioimpedance dependence of blood vessel volume change, which is caused by blood flow, and structural changes of whole blood will be studied. Several articles were found and analysed in current chapter with similar simulations of blood flow in the aortic to radial cardiovascular branch or parts of it.

The researchers from Lappeenranta University of Technology have provided two simulations [15], [16] to experiment and study wall share stress by simulating pulsatile blood flow through aortic arch and its branches. They used the same software, that was also used for simulation part of this thesis, within both studies. The dimensions were simplified and walls rigid. First study had two conditions hypotension and hypertension. The results showed that although the model was simplified, and walls were rigid they did get close to realistic expected results. The results prove that hypertension has impact on atherosclerosis by analysing low and oscillating wall shear stress areas where plaque growth will intensify. In second work they studied wall shear stress with different pulsation strength. In addition to main task of this work the WSS parameters will be studied and compared with these studies.

Denmark researchers used simulation of aortic arch to study aneurysm and possible approaches to restore the proper blood flow in the arch [17]. They also made simplified model of aortic arch with three branches and experimented with making the arch wider and interconnecting the branches between each other as cure for arch widening diseases. The results prove that hemodynamics get worse with aneurysm and can be cured with hybrid total aortic debranching.

D. Afkari has written a PhD thesis [18] about pulsatile blood flow interaction with arterial walls of aorta. In depth he describes pressure boundary condition and its biomedical applications using a 3D simulation of pulsatile blood flow in aortic arch. He implemented autoregulation and impedance to outputs instead of numerically set pressure outlet which gave more realistic results and direct feedback to inlet.

All the simulations of blood flow were done using model of aortic arch with three branches and only one article had interest in pressure waveform distribution and analysis. Others explored wall shear stress and only within the aorta. This makes the experiment described in this thesis novel and different. No simulations can be found that have aortic to radial cardiovascular system branch under study.

3 Anatomical background – Cardiovascular system

Cardiovascular system (figure 1) consists of heart, blood vessels and blood. Heart is one of the hardest working organs which can pump up to 35 liters of blood per minute in athletes during intense exercise. Vessels carry the blood from heart to lungs in first and from heart to every cell in the body in secondary loop of the system. Together with blood nutrients, oxygen, hormones and cellular waste products are transported all over the body [19], [20].

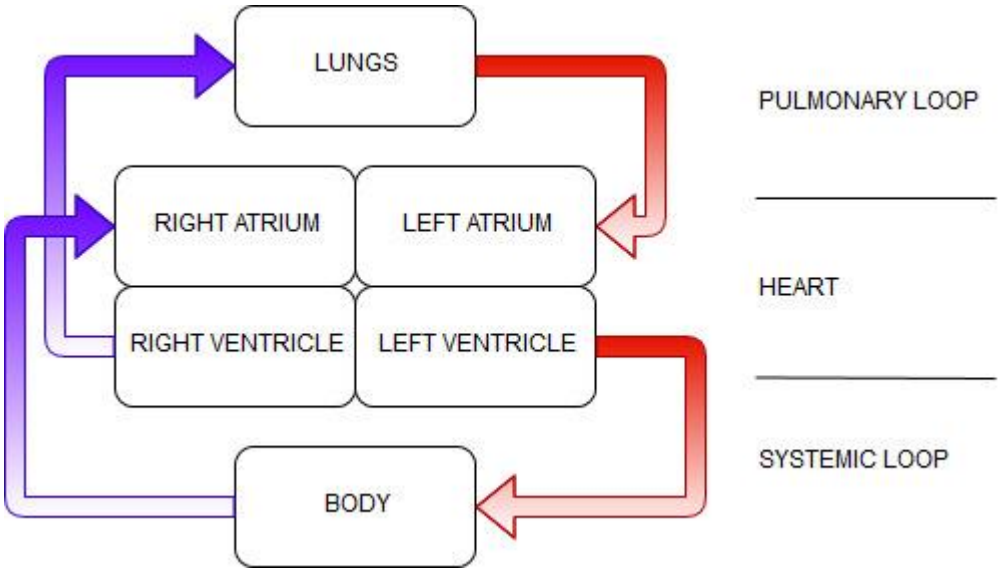

Figure 1. Cardiovascular system overview.

Systemic circulation loop is the second loop of the cardiovascular system which transports oxygenated blood from the left ventricle of the heart by arteries to different tissues of the body and returns deoxygenated blood back by veins to the right atrium [21].

3.1 Arteries

In a systemic circulation loop, arteries carry oxygenated blood from heart to all the tissues in the human body. The tree of arteries starts directly from the arch with the biggest blood vessel aorta. Big arteries face high levels of the blood pressure as the pumping motion of heart pushes blood flow with great force. Because of that the biggest arteries have thicker,

more elastic and more muscular walls than other vessels. Muscles of the bigger arteries contract to accommodate the high pressure of the heart.

Smaller arteries are more muscular in structure, but their task is to regulate the flow by contracting. By regulating blood flow, they also regulate the pressure which is proportional to change in flow because of change of the cross-sectional flow area. At the end of arteries there are arterioles which carry blood to the capillaries connected to tissues. There is huge number of arterioles that is why in them the pressure is much lower. Similarly, as arterioles, they regulate the flow with smooth muscles [19].

3.2 Aortic-radial blood transport

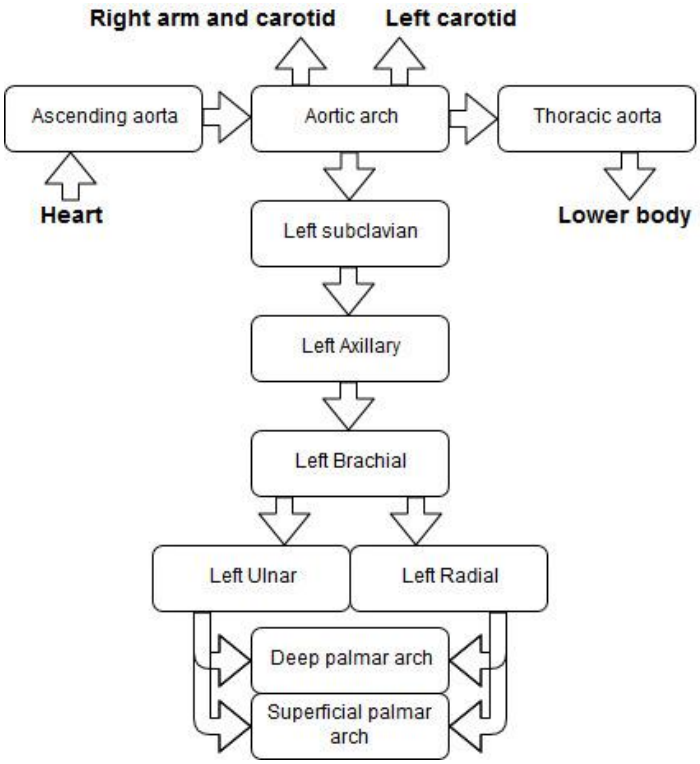

Figure 2. Aortic-radial blood transition path.

Aortic to radial blood transition path (figure 2) starts with aortic arch. It bends between ascending aorta coming from left ventricle and ends with descending aorta where from starts the blood supply path of lower body. Three branches are starting from aorta to supply upper body: left subclavian, left carotid and brachiocephalic arteries [21].

Upper body limb supply has five main vessels: subclavian, axillary, brachial, radial and ulnar arteries. Left subclavian artery has direct connection to aorta which why aortic to radial path is rather preferred the left side of upper body limb. Subclavian artery runs straight towards axillary artery. Axillary artery then continues to brachial artery after which has some smaller branches of arteries to supply upper arm. Brachial artery is divided to two forearm arteries radial and ulnar. In the end these arteries form arches that supply the hand with the blood [22].

3.3 Blood

Average volume of blood in human body is 4-5 litres. Blood has a liquid connective property which allows it to transport nutrients, cellular wastes and oxygen through the whole human body. Blood consists of following particles: red blood cells, white blood cells, platelets and liquid plasma.

Almost a half of blood volume are red blood cells which are transporting the oxygen through haemoglobin. Small part of volume is taken by white blood cells which play a significant role in human immune system. Platelets are responsible for clotting of the blood and plasma takes other half of volume and its function is to hold proteins and different substances like antibodies, albumins etc [19].

4 Bioimpedance basics

In this work bioimpedance of blood is under study. Bioimpedance measurement is analysation of tissue electrical properties when then electric current flows through it. Bioimpedance is the property of tissue to resist the flow of electric current [23] and store electrical charge [24]. Based on this the main properties to describe bioimpedance are electrical resistance and capacitance. Bioimpedance is complex number and following equation (1) describes the parts of complex bioimpedance Z:

$$Z = R + jX \tag{1}$$

where R is resistance and X reactance. Unit through whole equation is Ohm. Electrical resistance depends on the material ability to oppose the current flow and has same effect on AC and DC currents. Reactance depends on the frequency of induced current and opposes the current flow by accumulating the charges and discharging. Reactance is only present with AC currents. Reactance decreases with higher frequencies [25]. Following equations (2) and (3) describe the resistance and reactance dependence and evaluation.

$$R = \frac{V}{I} \tag{2}$$

Where V is voltage and I current like in the Ohm's law.

$$X = \frac{1}{2\pi f C} \tag{3}$$

Where f is frequency of excitation current and C is capacitance.

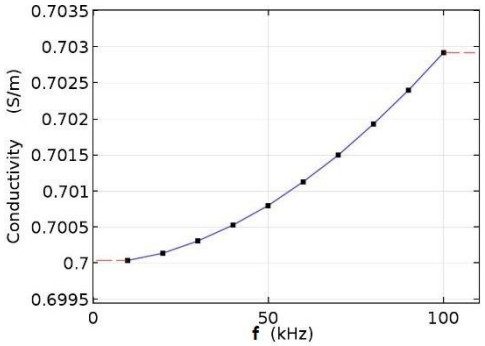

Figure 3. Whole blood conductivity change with different frequencies.

Figure 3 shows dependency of conductivity to frequency. For bioimpedance earliest founded and mostly used analysis method is single frequency bioelectrical analysis (SF-BIA). Used single frequency is 50 kHz. This frequency has good permittivity over most of the bodily materials and due to many times higher frequency of the blood pulsation the blood can be analysed as stationary [26].

4.1 Causes of bioimpedance variation

As described before blood consists of particles cells and wastes and plasma as connecting fluid. Solid particles of blood, the red cells, have high resistivity and plasma is a conducting fluid. Other contents of blood are not considered in bioimpedance measurement due to small size or consistency number [27]. Based on this knowledge the whole blood resistivity and conductivity changes with ratio of solid to fluidic parts of whole blood. Equation (4) describes this relation.

$$\sigma_b = \frac{\sigma_p}{1 + C\frac{H}{1-H}} \tag{4}$$

Where σ_b and σ_p are conductivities of whole blood and blood plasma respectively, H haematocrit value and C is the function of a/b where a is short and b long axis of erythrocyte. The higher is the consistency of plasma the higher is conductance of whole blood and vice versa. This is considered if there are no blood structural or vessel volume changes. Dependence on haematocrit value will be proven by simulation.

Measurements from study [28] measuring radial artery motion using photoplethysmography and pulsimeter, show that arterial artery has diameter change relation to flow velocity. The higher is the blood velocity the bigger is the volume of the vessel. Electrical resistance of measured body decreases with increase of volume according to following equation (5)

$$R = \frac{l}{\sigma_b A} \tag{5}$$

where l is length of the measured body, σ_b conductance of material and A the cross-sectional area. Impedance dependence on volume change will be executed in simulation.

There is a theory that one cause of impedance change of flowing blood are changes of orientations of red blood cells. Impedance of stationary blood does not change and is isotropic. Orientation of red blood cells in stationary blood is random based on Brownian motion. During applied high flow forces during peak pulse the blood cells are suggested to be oriented in alignment with flow resulting bigger cross-sectional area of plasma. Due to complexity of implementing orientation change of red blood cells in whole blood it would not be present in simulation [29].

4.2 Bioimpedance measurement technique

Charges are carried by ions in the body and electrodes are used for measuring bioimpedance. Most common electrode measuring technique for bioimpedance is four electrode type sensing, same as tetrapolar and Kelvin method. It is suggested to be most accurate because of the exclusion of current inducing leads resistance [23]. In case of using four electrodes for measuring the useful measuring frequency band is 0.1 to 100 kHz.

Two electrodes are used for current injection and other two to measure the resulting voltage drop. Since no current goes through voltmeter the electrode to body interface does not have influence on measurement. Simple four electrode sensing scheme can be seen on the figure 4 below [25].

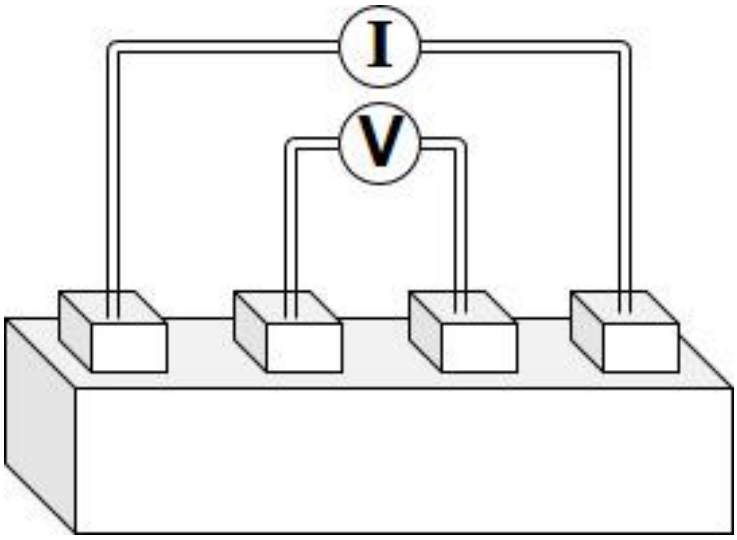

Figure 4. Four electrode sensing technique setup.

5 Blood flow physics and mathematical equations

Blood is a fluid that is mostly liquid because of the high consistency of liquid plasma which contains proteins to transport other solid contents of blood, which make viscosity of blood higher that the water [30]. To understand the physical background of pulsating blood flow properties the background of physics was researched. Simulation will consist of rigid volume and borders of blood transition lines with dynamic pulsatile flow of blood similar liquid. Fluid "similar" to the blood will be used because blood is not completely liquid and consists of solid cells and other particles.

Table 1. Blood consistency.

Content	**Mean percentage (and range) (%)**
Plasma	55 (50-62 depending on red blood cell amount)
White blood cells and platelets	1 (stays the same with every gender)
Red blood cells	44 (37-43 in women and 43-49 in men)

Flow dynamics is popular applied science branch and it is widely used in many different study fields and is widely used for studying the blood circulation. Flow dynamics describe fluidic properties and forces that affect the flow [31]. The study of flood properties of the blood is called hemorheology. Further in this chapter constants of fluid properties are described and dynamic properties that are related to flow and applied forces.

5.1 Liquid properties

Blood is non-Newtonian fluid, because of its viscoelasticity caused by elastic behaviour of red blood cells [32]. When blood is modelled in medium to large sized arteries the blood can be given properties of viscous, incompressible Newtonian fluid. Non-Newtonian behaviour of blood is only related to flow in arterioles and capillaries where

the size of the cells and particles of blood become comparable to the size of blood vessel [33].

Viscosity shows how much resistance a fluid propagates against the deformations caused by external forces and is directly related to internal friction of molecules in the fluid. In everyday use it is called “thickness” of the fluid. The smaller is the viscosity the higher is the fluidity of the fluid [34]. Measured dynamic viscosity of blood at 36 degrees Celsius is approximately 5 mPa*s [35].

Compressibility of fluid means that that density of the fluid changes because of the applied external forces. Study related to compressibility relation to the density of blood reported that the blood is compressible fluid and it depends of consistency of blood [36]. Although the consistency of blood changes within longer period than is the simulation duration the blood can be given constant density. Standardized density of whole blood is approximately 1060 kg/m3 [37].

5.2 Flow properties

Blood flow can be described by following parameters the velocity, pressure and pulsation. Blood flow starts with pulse impulse which is produced by heart and blood travels by vessels through the whole body. Pulsation can be felt mainly across medium to big vessels. In small vessels pulsation is not consistent anymore.

In this thesis simulation, the flow is simulated only in aortic to radial arteries, which are medium-large sized, where flow is pulsating. All the following parameters are implemented in the simulation with most possible precision and reality.

5.2.1 Velocity

Velocity describes distance which blood travels in unit of time. It is not same as with the flow, because flow describes the amount of blood moving through cross-sectional area in unit of time. Narrowing of vessel output increases velocity but flow remains the same. Velocity changes from aorta to capillaries approximately from 20 m/min to 1.6 cm/min, if considered that cross-sectional area of aorta is 2.5cm^2 and all the capillaries in the body 3000cm^2 and blood flow through vessels is 5 l/min. Following equation (6) describes flow velocity:

$$V = \frac{Q}{A} \tag{6}$$

Where Q is flow rate and A cross-sectional area of the vessel(s). Change in velocity is caused by flow resistance of vessels that gets higher with narrowing of vessels during the blood travel paths. Capillaries have large flow resistance to slow down the velocity of blood to exchange needed particles consisting in blood with tissues [38].

5.2.2 Pressure

Pressure describes the force per cross-sectional area that is applied on the fluid for maintaining flow or motion. Pressure SI unit is Pascal (Pa) but in medicine the millimetres of mercury (mmHg) is used. One millimetre of mercury is equivalent to 133.322 Pascals of pressure. Equation (7) describes pressure evaluation, where F is applied force on A size cross-sectional area [39].

$$P = \frac{F}{A} \tag{7}$$

Sometimes the flow of blood is described with energy parameters according to equation (8). Blood is flowing based on the sum of kinetic energy and pressure energy and the sum should also remain the same (figure 5). The whole energy is energy that is used to deliver some blood amount from one point to another [40].

$$E = KE + PE \tag{8}$$

Where E is total energy, KE is kinetic energy or velocity squared and PE pressure energy.

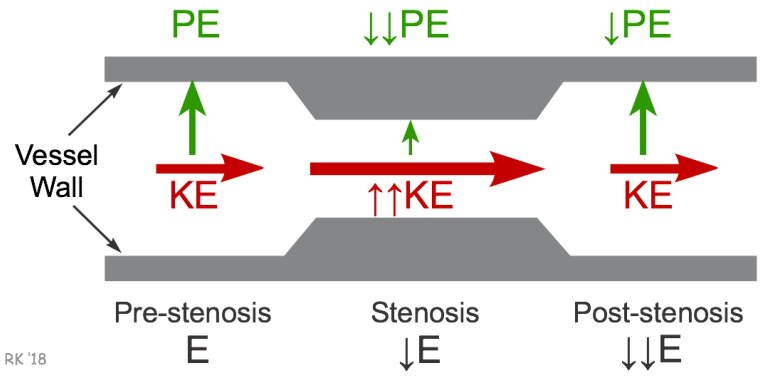

Figure 5. Energy distribution of blood flow in a vessel [41].

According to Bernoulli's principle pressure and velocity are related between each other. If the velocity increases the pressure decreases, for example during narrowing of blood vessel and returning to normal size. During the narrowing the pressure decreases, and

velocity increases and in the widening it gets back to the values that were in the beginning [41]. Principle can only be applied to one short time period and part of circulatory system because principle has restriction in steady flow.

5.2.3 Pulsation

Since heart is beating and providing impulses to maintain blood flow, there is pulsation in both velocity and pressure, visualized in figure 6. Pulsation is present in all the vessels in aortic to radial blood transition path. The pulsation grows for both pressure and velocity with opening of left ventricular valve and descends when valve is closed. During the closed valve pressure grows in the left ventricular for blood to be pushed out of the heart [40].

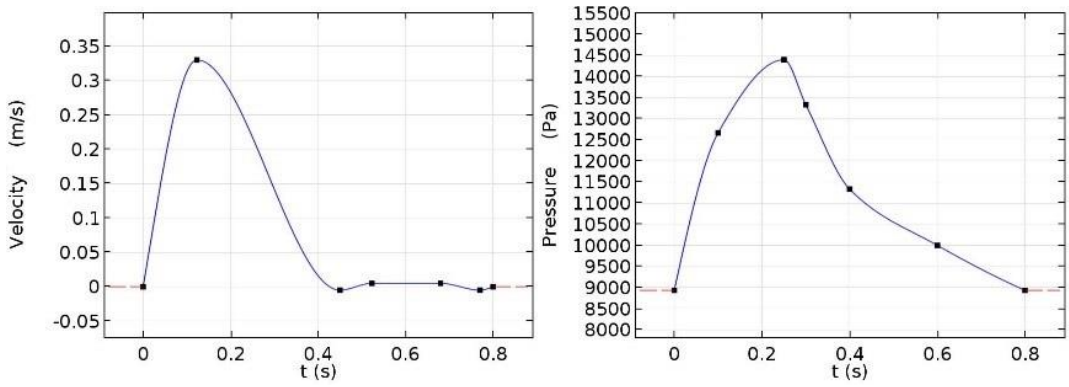

Figure 6. Presence of pulsation in velocity and pressure waveforms from aorta.

5.2.4 Aortic-radial blood pulse transit time

Pulse transit time (PTT) describes the time that is needed for pulse to be transmitted from aorta to any peripheral artery. The measurement and estimation of PTT is taking pulse waveform from 2 different places and measuring the time difference from one signal foot to the next. PTT also describes the pulse wave velocity because we know the distance travelled and time interval that the transition took. Article related to PTT measurement had aortic to radial pulse transition time of 0.08 seconds [42]. This parameter is useful for simulation to get flow operating properly from aorta to radial artery.

6 Modeling

Aortic to radial model was made using Autodesk AutoCAD 2017 software. The model was made in 3D with centre of cross-sectional line made straight plane. Model has lots of simplifications, parameters like curves, diameters of arteries and length are close to realistic based on mean measurements collected from the web resources. Final model was made union solid and later called “blood”.

During the drawing of the model the curves and dimensions were gathered together. By following anatomical logicality, making approximate assumption and analysing personal body the model was drawn. The detail and correctness of the model has a lack in lots of curves and dimensional changes compared to realistic system. Significant approximations and implications did not become a problematic side since the fact that the more detailed model would be the longer the computational time would be, and model adaption difficulties would be present in the simulation software. The main dimensions of the arteries were gathered together from trustworthy sources, also the blood path model was consistent with the illustrations and human body scans from the same sources. Final model was rated acceptable.

Complete model (figure 7) based on parameters described in chapter 6.1 was a result. In the picture there is also a frame which on the complete model was based on. Frame is useful to, if needed, change the size parameters of the model in the future.

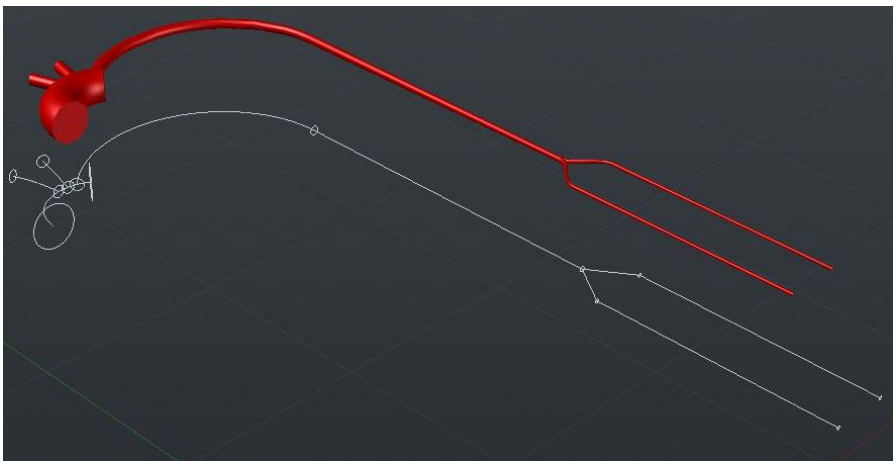

Figure 7. Constructed frame and solid model.

Next figure 8 has naming of all the arteries that are present in aortic-radial blood transition path.

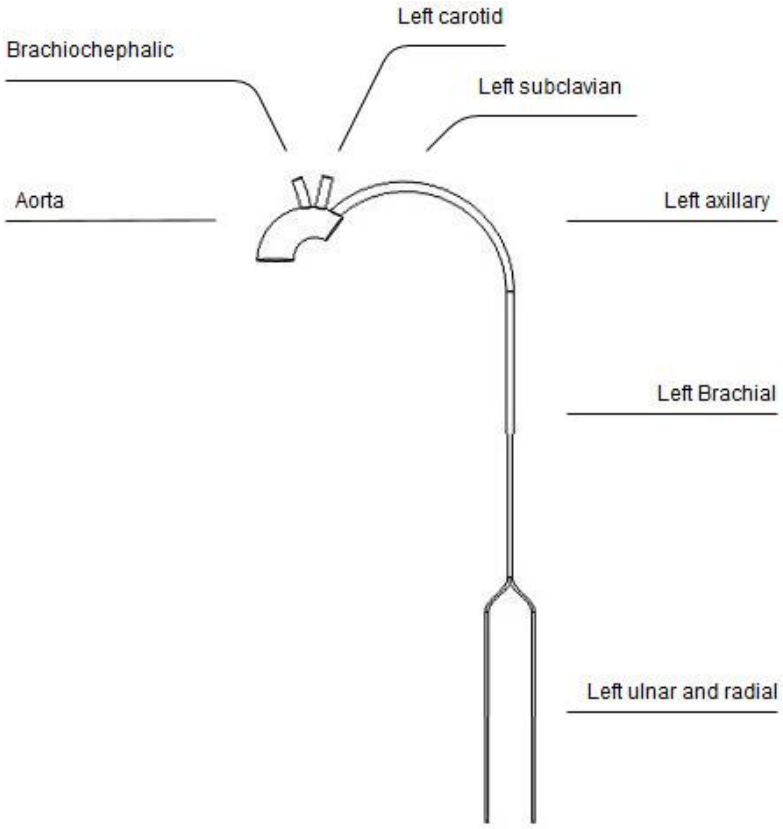

Figure 8. Arteries included in the model.

Base functions that were used:

Circle -start and end of arteries, uses centre point and radius for drawing a circle, angle of circle with path line was always chosen perpendicular with 3-point line.

3-point line – drawing path lines, uses 3 points for drawing a line. Start-curve-length and start-curve-end type 3-point lines were mainly used.

Loft function – to make smooth connection with start and end circles and follow the path line.

For combining arteries to one complete solid, functions like union, subtract, interfere, separate and convert to solid were used.

6.1 Dimension parameters

For 3D model drawing length, start-end inner diameter and curve angle had to be gathered for each individual artery. Parameters from different sources [43]–[53] were gathered together and mean values used. Parameters from one individual would be better solution but all analysed sources with complete dimensions were not so trustworthy. Lack of sources with complete dimensions of human body can be due to prohibited human autopsy and no perfect scan tools to analyse all the dimensions of the one individual human body, making a difference between all the tissues.

Table 2. Dimensions of vessels.

Blood vessel	**Internal diameter (mm)**	**Used value for diameter(mm)**	**Wall thickness (mm)**	**Length (used value) (mm)**
Ascending aorta	25.8 - 37.6	Start 31.7	2	30 (30)
Aortic arch	20.4 - 28.4	End 24.4	2	40 (40)
Subclavian	6 - 12.8	Start 9.4	1	90 (90)
Axillary	5 - 8	End 6.5	1	100 (100)
Brachial	3.4 - 4.4	6.5-3.9	1	205-290 (245)
Ulnar	2 - 2.8	3.9-2.4	1	190-240 (215)
Radial	1.9 - 2.7	3.9-2.3	1	190-240 (215)

Later left carotid and brachiocephalic artery beginnings were added to the arch as was discovered they were needed for pressure compensation of the arch.

Table 3. Brachycephalic and carotid artery beginnings dimensions.

Blood vessel	Internal diameter (mm)	Used value (mm)	Wall thickness (mm)	Length (used value) (mm)
Left carotid	8.5 – 8.8	8.8	1	28 (28)
Brachiocephalic	8.80	8.8	1	28 (28)

Table below also describes some additional values that were used during drawing the model.

Table 4. Additional dimensions.

Parameter	Radius (mm)	Distance (mm)
Aortic arch curve radius	32.5	-
Shoulder curve radius	90	-
Distance between radial and ulnar artery	-	40

6.2 Simplifications

Model is in 3D and the size is close to realistic by length and curvature not only in planar placement of vessels, the centre of model is lying on xy-plane. Restriction of model poor detail were applied only because of the meshing difficulties from simulation software. Corners of model were made sharp because the simulation software could not build mesh with rounded and filleted edges. Also branching is sharp because of the same problem of simulation software “Coarse” quality meshing. COMSOL adapts detailed CAD models to its interface and cannot repair them so the relative repair tolerance number is between limits. Non-rounded and -filleted edges do not give that error. Other solution instead of removing rounded and filleted edges is making mesh quality finer but it dramatically increases computational time.

7 Setting up the simulation

For simulation the computer-aided engineering (CAE) software was needed with possibility to simulate electric current flow and that had computational fluid dynamics (CFD) module. Because fluid dynamics are complex and cannot be solved by direct calculations the CFD study should be used [31]. COMSOL software suited well because of its wide variety of integrated modules, simulation possibilities, and authors previous experience of using this software for providing simulations.

Practical work of this thesis mainly was done in CAE software only the model was imported from CAD software because of COMSOL lack in possibilities of CAD drawing tools compared to AutoCAD software. Defining material properties, adding physics and evaluating measurement results were all done in CAE software and described further in this chapter.

After importing the CAD model, the whole geometric entity was given blood material properties. Afterwards for arterial wall elasticity and bioimpedance measurements simulation the arterial wall was added to the radial part of the model and electrodes placed. After geometries were fixed and all the needed parts added and formed into union every separate domain was given the physical properties (Table 5) that were needed for properly working physics.

Table 5. Material parameters

Property	**Value and unit**
Density of whole blood	1060 kg/m^3
Dynamic viscosity of whole blood	0.005 $Pa \cdot s$
Electrical conductivity of whole blood @50kHz [54]	0.7008 S/m

Relative permittivity of whole blood @50kHz [54]	5197.7
Young's modulus of the radial artery wall [55]	6 MPa
Poisson's ratio of the radial artery wall[56]	0.45
Density of the radial artery wall [55]	1000 kg/m^3
Electrical conductivity of the radial artery wall @50kHz [54]	0.31686 S/m
Relative permittivity of the radial artery wall @50kHz [54]	1633.3
Electrical conductivity of electrode [57]	10 S/m
Relative permittivity of electrode[57]	11.2

From CFD module laminar flow physics was chosen. Laminar flow simulation is used to compute the velocity and pressure fields for the flow. The laminar flow stays laminar until Reynolds number is below the critical value. When Reynolds number exceeds critical value, the flow becomes turbulent and is also simulated within this physics setting. COMSOL Laminar flow interface uses Navier-Stokes equations and continuity equation for momentum and mass conservation respectively [57].

Reynolds number is dimensionless parameter that predicts the fluid behaviour patterns. It is used to foresee if the flow will be laminar or turbulent. Reynolds number is ratio between inertial and viscous forces. If inertial forces are dominant the flow is turbulent and vice versa. The critical Reynolds value for internal flow of a pipe, or a vessel, is 2300. Reynolds number is evaluated in COMSOL based on following equation:

$$Re = \frac{\rho V D}{\mu} \tag{9}$$

where Re is Reynolds number, ρ is the density of the fluid, V the velocity of the flow, D the diameter of the pipe, vessel in this case, and μ the dynamic viscosity [58].

COMSOL uses following Navier-Stokes equation to describe compressible Newtonian fluid flow [57]:

$$\rho\left(\frac{\partial u}{\partial t} + u + \nabla u\right) = -\nabla p + \nabla \cdot \left(\mu\left(\nabla u + (\nabla u)^T\right) - \frac{2}{3}\mu(\nabla \cdot u)I\right) + F \qquad (10)$$

Where u is the velocity, p is the pressure, ρ is the fluid density, and μ is the fluid dynamic viscosity. Left part of the equation are the terms corresponding to internal forces. And on the right pressure forces, viscous forces and external forces are defined. From viscous forces the following term can be removed:

$$-\frac{2}{3}\mu(\nabla \cdot u)I \qquad (11)$$

because for incompressible fluids the continuity equation yields:

$$\nabla \cdot u = 0 \qquad (12)$$

Boundaries were given wall, inlet and outlet properties. Walls of vessel were set rigid and boundary condition was set to “No slip”, because main effect of wall is to just stop fluid from leaving outside the domain. The inlet was given velocity waveform and outlets of vessels the pressure waveforms. COMSOL gives correct results only for condition as velocity for inlet and then pressure for outlet or vice versa. If condition is not met there will be convergence difficulties. Suppressing backflow property was also added for all the outlets to prevent fluid entering from outlet boundary.

Inlet and outlet waveforms were taken from other researches [59], [60] and imported to COMSOL using interpolation function with piecewise cubic interpolation and constant extrapolation type. Following figure 9 shows all the used waveforms.

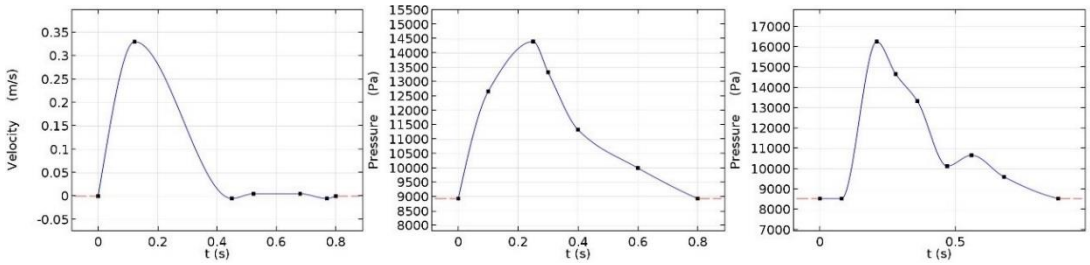

Figure 9. From the left: inlet velocity of aorta, pressure at outlets of aorta and its branches, pressure at the outlets of radial and ulnar arteries.

After setting up the flow the electric currents (ec) physics was added form AC/DC module. For the first electrode input potential was give of 1V and the fourth was set as ground. Probes were set on first electrode to measure induced current and on second and third electrode to measure voltage to find the potential difference between them.

As final physics the solid mechanics physics (solid) were added from structural mechanics module. The arterial wall was given properties of isotropic elastic material. For simulation evaluation the mesh should be mobile, so the moving mesh module was added and specified all the boundaries that are fixed or flexible. To get interaction between the flow and elastic wall the fluid-structure interaction was added from multiphysics module. This way the flow forces had influence on the arterial wall making it wider or narrower.

Before evaluating the study mesh of the domain had to be built. Mesh element size was set coarse to make computation time shorter. Study properties were selected 50Hz sampling frequency with new sample data set every 0.02 seconds. Study was chosen time dependent and fourth pulse was analysed, because the pulsation can be unstable during first pulsations and becomes stable further on.

8 Results and discussion

The final version of simulation with setup described in previous chapter did not give any errors and evaluated properly. The complete mesh consisted of 108511 domain elements, 24252 boundary elements, and 1915 edge elements. Using personal computer, with hardware and software setup described in Appendix 1, the average computational time for the study was one hour. The process of changing variables and parameters and recomputing the solution was very time consuming due to very long computational time. Computational time can be reduced by making mesh quality coarser and increasing the performance of the used computer.

After every computation of results the first thing to analyse was overall functionality of the model by reviewing the pressure and velocity distribution animations of the last pulse. Animation was viewing the changes in longitudinal 2D cross-section of whole model (figure 10).

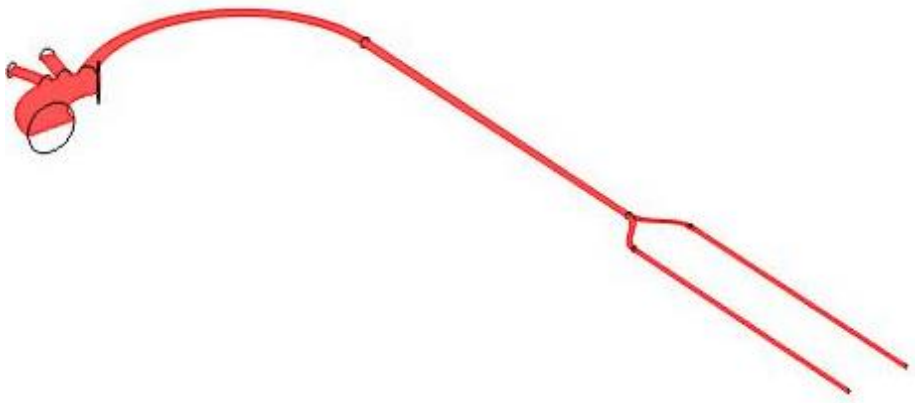

Figure 10. Result output cross-section to rate correctness.

Based on theoretical knowledge gathered together in the theory background part of this thesis, the solution was given a rating of correctness. Since the simulation main computed parameters over the mesh were pressure and velocity, the main properties analysed from animations were the pressure waveform in which the amplitude should get bigger and velocity magnitude should decrease with propagation away from the aorta inlet within pulse transit time. In addition, the pulse wave should move away from the inlet towards

output, so the flow is only monodirectional and no backward flow is present, although the inlet velocity sometimes goes to negative value which means short inverse movement of blood caused by closing of the heart valve. It only causes the inverse flow with pressure drop at the inlet and has no effect on the overall flow direction in the system.

In following figures, the best suitable set of results outcomes and with most reliable correctness based on animation analysis is visualized. Figure 11 shows pressure and velocity distribution in aortic arch and its surroundings during systolic peak. Amplitude of pressure increases and velocity decreases after going out from aortic arch. Velocity increases at the end of ulnar and radial artery because there are no additional vessel branching in the arm path which would stabilize and decrease the output velocity at the forearm. In the lower part of the arm velocity acts as default propagation in decreasing tubes where flow rate remains the same but the velocity increases. And in figure 12 there are two time points of systolic peaks in aorta and forearm vessels. The pressure pulse propagates from aorta to radial and ulnar arteries in 0.08 seconds referring that the flow is towards outlets with correct PTT value described in Chapter 5.2.3.

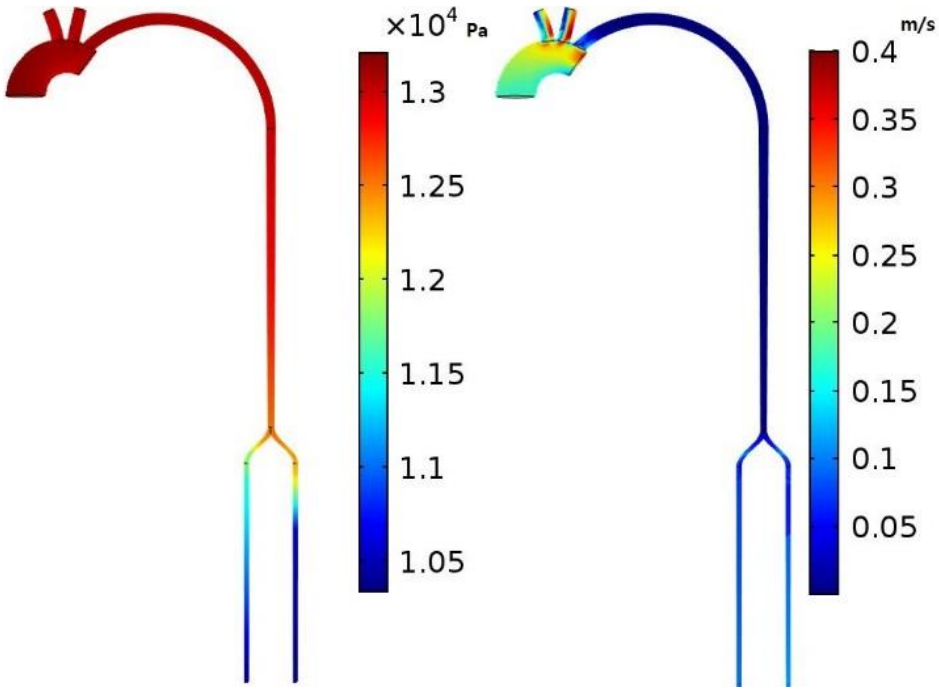

Figure 11. Pressure and velocity distribution at systolic peak (t = 2.61 s).

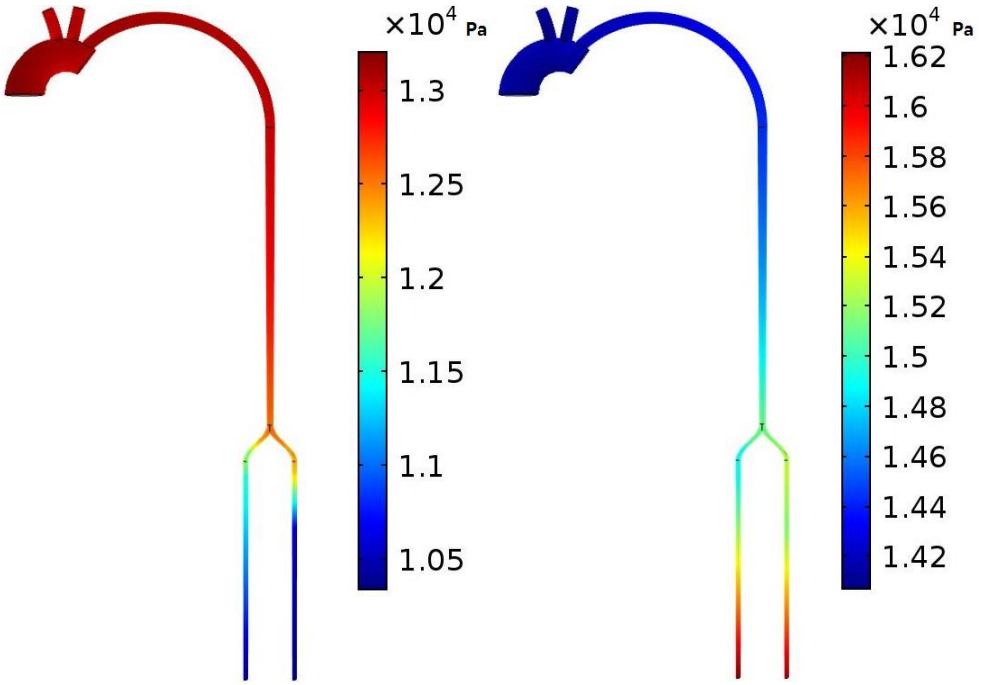

Figure 12. Pressure pulse propagation from aorta to end of forearm in 0.08s (t = 2,52 s and t = 2,60 s).

During next chapters the 5cm part of the radial artery from the whole model will only be shown in figures and its location is on the model 2.5cm above the end of radial artery. This is the part where the four electrodes for measurements are placed with 1cm distance between them. Location and used segment itself can be seen in Figure 13. This was done to zoom in to the part of the interest and decrease the computational time. Every parameter of the segment, like input, output, material properties, and others, are the same as they would be in the complete model.

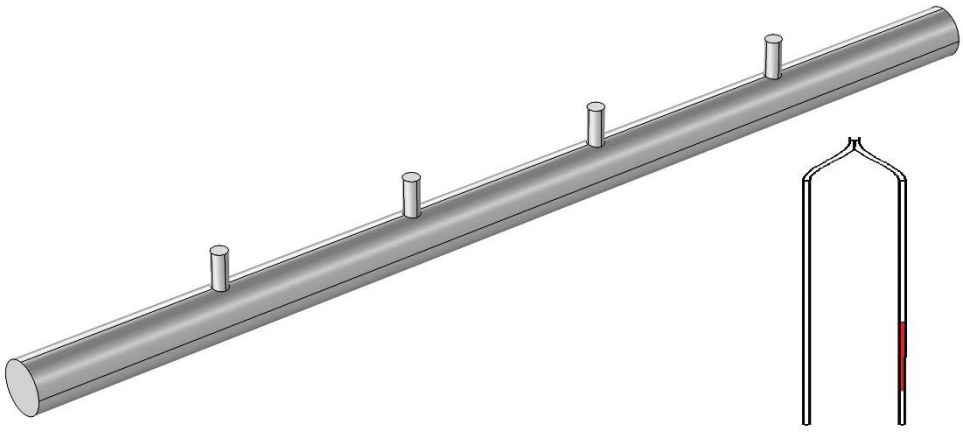

Figure 13. The segment of radial artery with electrodes and its placement on whole model.

Simulation results will describe influence on bioimpedance measurement variance caused by consistence of blood, the haematocrit ratio and dimensional changes caused by pulsatile blood flow. SF-BIA will be provided with corresponding electrical properties of blood. As a last thing WSS will be analysed and compared to researches from Finland described in the chapter 2.3. All the results will be analysed and discussed with use of knowledge of theoretical background and authors personal ideas and thoughts.

8.1 Impedance vs blood structural changes

Measured impedance of steady blood and flowing blood did not give any difference (figure 14). Since fully liquid blood similar fluid is used to simulate whole blood, instead of mixture of solid particles in the liquid plasma, the impedance would not have any changes between steady and flowing blood simulation. Electric current conductance in this case has no influence from flowing liquid.

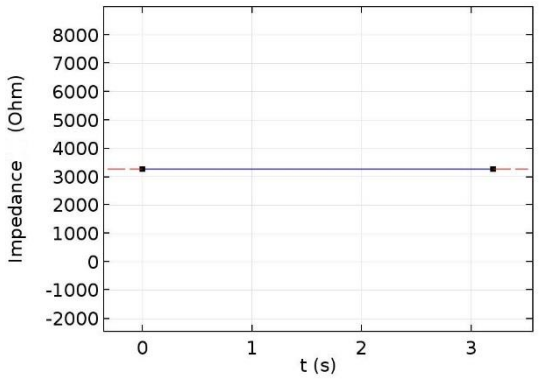

Figure 14. Blood flow bioimpedance measurement result in rigid tube.

According to these measurements, change in orientation of red blood cells, described in chapter 4.1, and other fluid structural changes can be the cause of flowing blood bioimpedance change but not the flow itself. These changes are difficult to implement and can only be studied independently because of the lack in tools of COMSOL simulation software and possible very high computational time due to high complexity.

Another cause of steady blood bioimpedance change is due to haematocrit ratio. Grownup human normal haematocrit value range is 37-49% depending on sex, age and individual physiological properties but it can be lower and higher because of different abnormalities. Following figure 16 shows the dependency of haematocrit to conductivity based on

equation 4 discussed in chapter 4.1, where the plasma conductivity is taken 1.57 S/m and the erythrocyte axis a and b ratio C 1.91 [28]. From the figure it is seen that healthy haematocrit consistency in the blood would keep the conductivity of whole blood between the 0.5 and 0.8 S/m range. Based on this experiment impedance measurement can be used for blood consistency analysis.

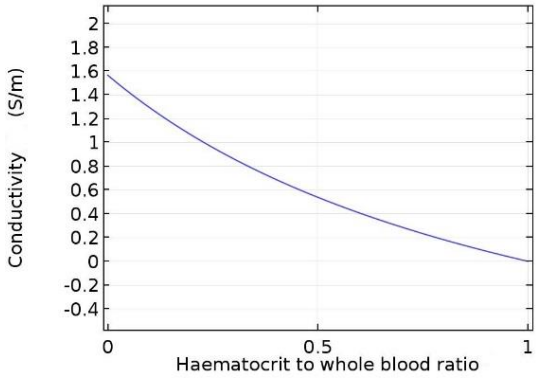

Figure 15. Conductivity depending on red blood cell volume to whole blood ratio.

8.2 Impedance vs volume

The measurement of the blood resistance in the radial artery was provided depending on volume change and compared to the one theoretically computed results based on equation 5 from chapter 4.1. There is an offset between the results approximately -0.33% which can be seen in Figure 16. It may be caused by round electrodes which make the vessel volume length between them not exactly 1 cm long. Regarding the offset the changes present in simulation are consistent with the ones evaluated theoretically.

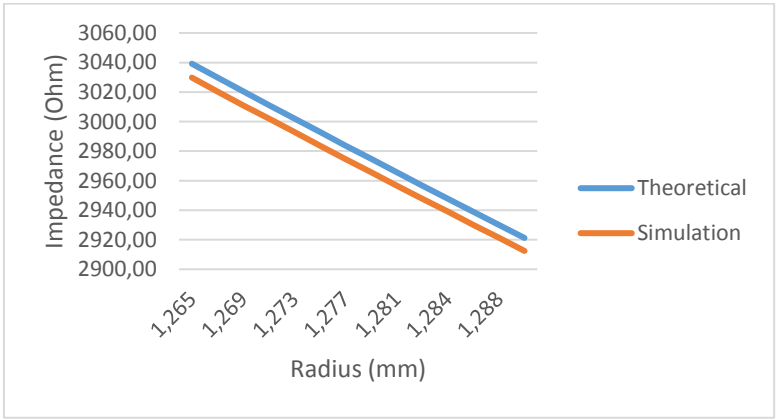

Figure 16. Comparison of the theoretical and simulation-based impedance change with vessel radius.

Impedance depends on the volume change. Knowing this the elasticity waveform of the vessel can be extracted from impedance measurement and from there the velocity waveform which causes the vessel wall to stretch out in the rhythm of pulsation. If the elasticity of the vessel had linear relation with velocity change the impedance measurement from pulsating vessel would be like in the figure 17. Oscillation in this case was 3%.

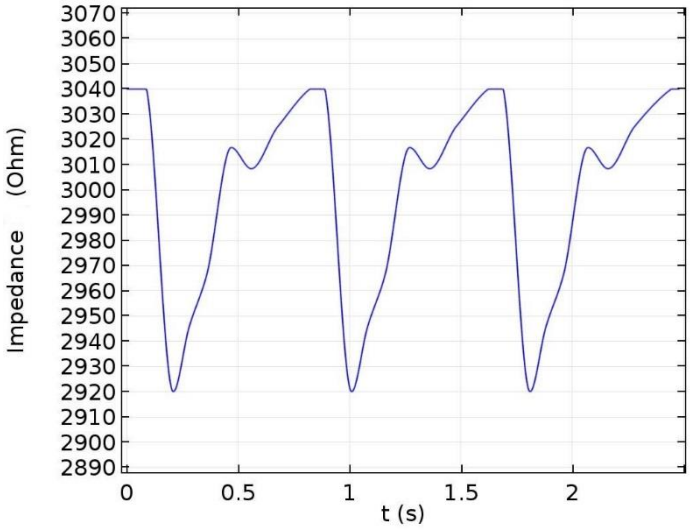

Figure 17. Impedance measurement result if the vessel dimensions would change linearly with the change in blood pressure.

Unfortunately, the elasticity of the blood vessel does not have linear relation with pressure nor velocity change. More detailed study was carried out to simulate the pulsation in the elastic arterial wall depending on pulsatile flow. Since COMSOL Multiphysics 5.2 lacked in tools the version 5.4 was found to be more suitable and could be used instead. Newer version had fluid to mechanical interaction and moving mesh modules which allowed to build a vessel with dynamic wall movement.

2D axis-symmetric geometry was used and the 5 mm long part of the radial artery with electrodes can be seen in figure 18. Smaller part of the vessel was used in the next experiments to continue decreasing computational time and performance resources needed for evaluation of results. Electrodes are bands surrounding the vessel and this kind of placement was chosen due to 2D axis-symmetric geometry type.

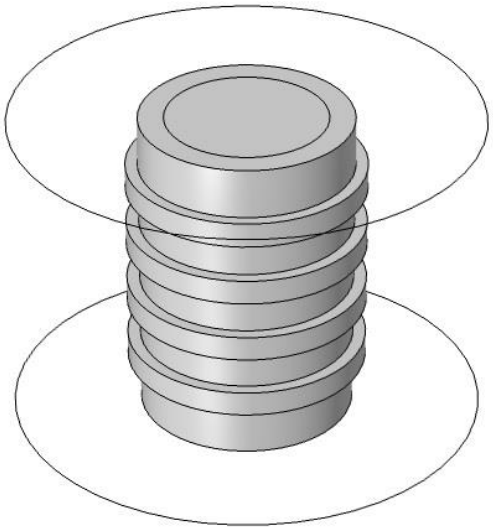

Figure 18. Electrode placement on artery and visualization of studied vessel segment.

The simulation of flow caused stretching of the arterial wall was successful and the minimum and maximum deformations can be seen in the figure 19. At the start of the simulation the model fills itself up and after does not go below the minimum because of the pressure in radial artery is present constantly. Although sides of the model are fixed in motion the motion within sensing electrodes is significant and impedance measurement can be carried out.

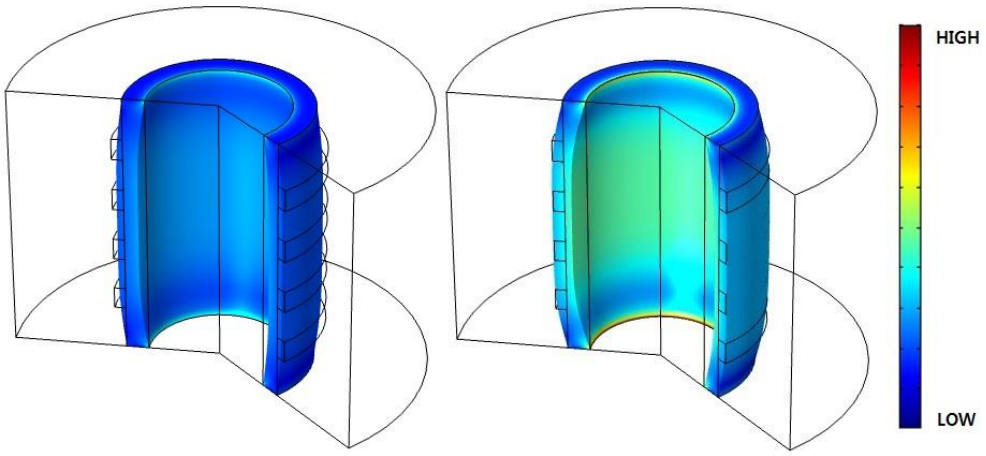

Figure 19. Minimum (t = 1.48 s) and maximum (t = 1.68 s) stretching deformations of the radial artery wall caused by pulsatile blood flow (with internal forces in colour).

By measuring induced current from the first electrode and potential difference between the second and third electrodes the bioimpedance could be evaluated by dividing electric

potential difference with induced current. Graphical representation of the result can be seen in following figure 20.

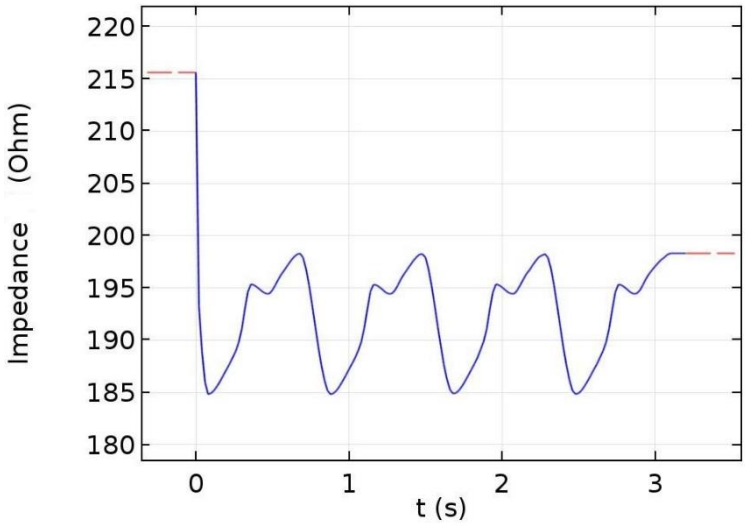

Figure 20. Impedance measurement result from the surface of pulsating arterial wall.

Impedance waveform measured by simulated radial artery motion caused by pulsating flow was convenient to the one where the deformation of arterial wall estimated to be linearly related to pressure change visualized in figure 16. In this case we see the fill-up of the artery in the beginning of the waveform and then 6% high oscillation comparing to the 3% that we got before. This means that diameter change of the artery does not have linear relation to the blood flow pulsation and depends fluid to structural interaction and elasticity of the arterial wall.

By making measurements through the length of whole arteria the remarkable changes in bioimpedance measurement that are not anatomically explained, by branching or dimension change, can indicate to abnormal deformation of arteria. Since the volume change has influence on measured bioimpedance value arterial diseases like aneurysm and plaque growth can be detected by making measurement analysis long the arteries. For healthy arteries change in the bioimpedance values should be smooth and explainable by anatomical dimensions of arteries. Next experiments were carried out to show how different abnormalities of the arteries are present in bioimpedance measurement results.

8.2.1 Aneurysm of arterial wall

To study aneurysm of the artery, the bulk was added having the form of the ellipse with the diameter 1mm in the middle and 1 cm long. The movement of electrodes was simulated over the deformation starting with centre of the bulk 0.5 cm and ending 4.5 cm away from the vessel segment beginning (left side on the figure 21). This was done to evaluate the best placement of electrodes for the best detection of defect.

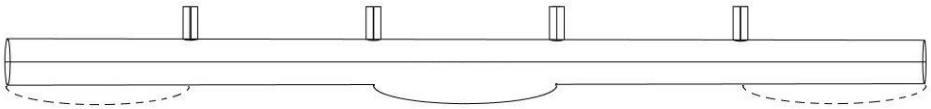

Figure 21. Aneurysm vessel defect and its start and end positions during measurements.

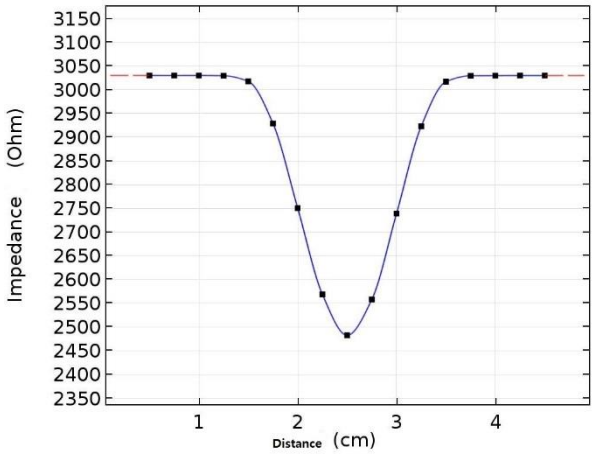

Figure 22. Measured impedance by moving electrodes over the vessel defect.

As we can see from the measurement result figure when the defect is exactly between the sensing electrode (second and third electrode) the impedance is at its minimum and increases when defect is moving away from sensing area. Based on this experiment the aneurysm can be detected if the expected value of the normal arterial bioimpedance value in this place is known. It is impossible to measure it as we do not know when it is healthy or not, but it can be estimated by analyzing the nearest areas to the measuring space. It can be a sign of vessel stretching or aneurysm if the impedance result is significantly decreased.

8.2.2 Plaque on arterial wall

To study plaque growth on arterial wall detection the arterial deformation was made only toward inside of the artery comparing to aneurysm (figure 23). The same size and placements were used for this experiment as in case with aneurysm.

Figure 23. Plaque vessel defect and its start and end positions during measurements.

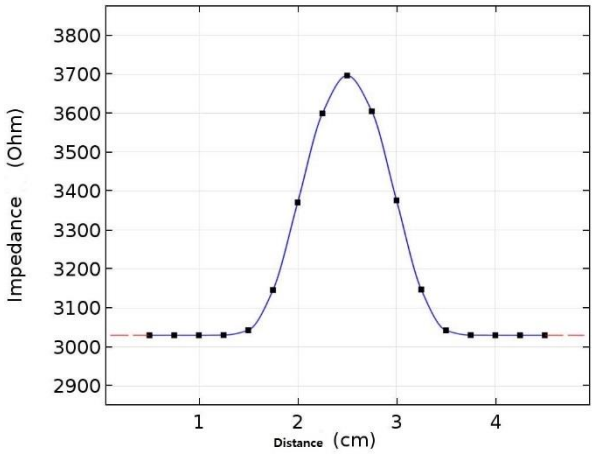

Figure 24. Measured impedance by moving electrodes over the vessel defect.

As seen from the results (figure 24) with increase of plaque built on the wall of arteria the measured impedance increases and reaches maximum value while the defect is between the sensing electrodes. Based on this experiment the plaque growth can be detected by impedance measurements and the sign of this defect would be a significant impedance increase compared to surrounding areas. Measurements done in this experiment and previous are provided from the surface of artery. Measurements from the surface of the skin will have noise in results and are not going to be so informative.

8.3 Wall shear stress

Wall shear stress was one of the results outcomes to compare the evaluated values to the previous studies described in Chapter 2.3. Wall shear stress study can help in foreseeing the intense plaque growth in some areas. Large arteries with significant curves like aorta

and its branches are suggested to be more vulnerable to atherosclerosis. The lower is the WSS the more intense can be plaque growth within this area. Following figure shows evaluated WSS distributions in the aorta and its branches. The colour legend is lowered to 0.5 Pa in maximum value to better visualize the lower range WSS distribution. Actual maximum is 5 Pa.

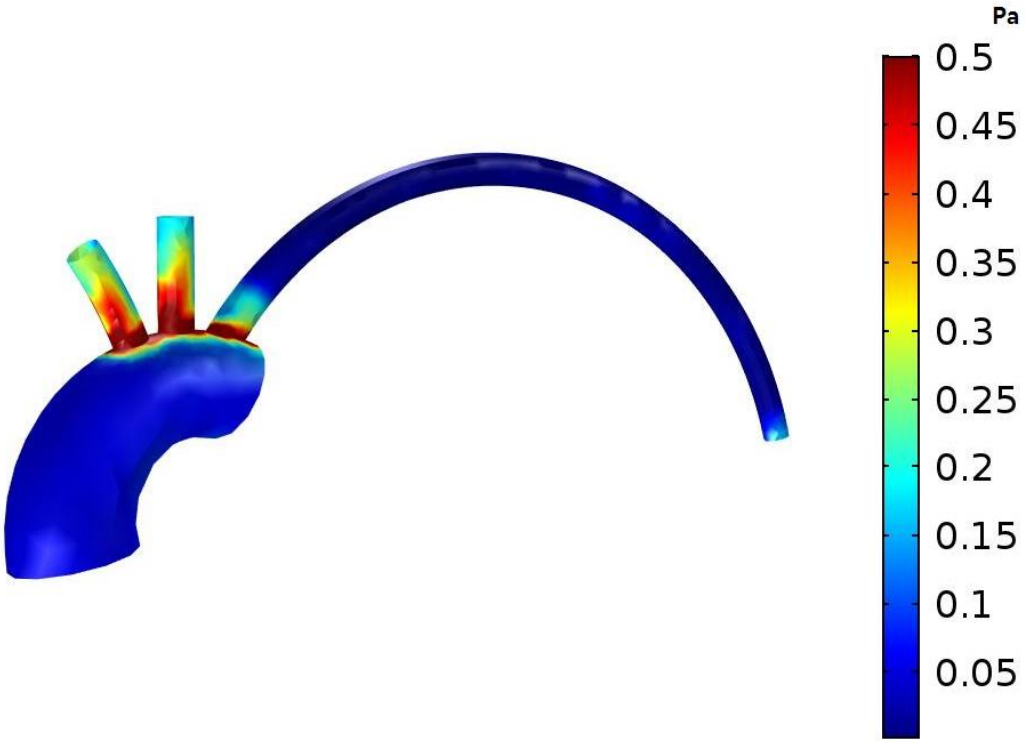

Figure 25. WSS distribution during peak systole t = 2.61.

Comparing to previous studies the vulnerable areas with low WSS are similar. Risk of developing atherosclerosis is in many places of aorta where WSS is low and oscillating. WSS is most high at the connection points of the aorta with the branches. This could be because of sharp and rigid connections. Also in this thesis the left subclavian artery reaches out to the forearm and from the WSS distribution and velocity distribution, figures 25 and 11 respectively. Outlet to left branch of aorta differs from others. Simulation may give more precise and different results with implementation of wall elasticity, filleted edges, wider model area and more details in model parts and branching, although the simulation is already consistent with previous studies of WSS.

9 Summary

Research in this thesis showed how cardiovascular system can be simulated using novel simulation software and practical outcomes of it. Simulation process is described from the modeling to result evaluation and discussion. Main goals of the thesis were to simulate a human cardiovascular aortic to radial blood transition path with pulsation and possible anatomical changes in structure and dimensions. In the simulation bioimpedance measurements, using four electrode sensing technique, were provided to get an overview between flow and impedance change relation.

Two parts were included in this study the theoretical and practical. In theoretical part basics of cardiovascular anatomy, physical background, bioimpedance sensing and state-of-the-art were reviewed, including literature analysis and base knowledge to provide the simulation. Experimental part described model, simulation and result evaluation based on gathered parameters and knowledge from literature. Results were analysed and discussed from perspective of authors experience, personal thoughts and suggestions.

Using aortic to radial blood transition path dimension parameters gathered together from the literature a 3D CAD model was drawn. Using this model successful simulation of pulsating blood flow was provided with implemented elastic changes of arterial wall and other geometry changes mimicking diseases like aneurysm and atherosclerosis. As an output impedance measurement, wall shear stress and blood conductivity change depending on haematocrit ratio to whole blood were evaluated. Animations of velocity and pressure distribution showed that simulation performed as intended.

With increase of haematocrit ratio to whole blood the conductivity decreased, which showed that whole blood consistency analysis is possible to provide using bioimpedance measurement.

By studying volume change relation to impedance measurement. The theoretical and simulation-based experiments showed that volume increase causes decrease in impedance. For further analysis the pulsatile blood flow interaction with elastic arterial wall was simulated which resulted in impedance change according to the results gathered

before. In impedance measurement result the motion of arterial wall can be detected, from where the pulsation waveform can be extracted. WSS study showed that with simple model with sharp edges and rigid walls development of atherosclerosis can be studied.

Whole blood consistency changes and CVD formation are long term changes in cardiovascular system and comparing to them pulsating flow caused changes are rapid. Simulation-based study showed that bioimpedance measurements are suitable for detection of short- and long-term changes in cardiovascular system. In real world this measurement is provided non-invasively and in the measurement results there are noise and disturbances from body to electrode contact and other tissues, between the surface of the body and arteries, with individual movement and physical properties which are not present in this simulation with ideal conditions.

For further analysis the model should be made more realistic or even patient specific with proper dimension parameter set from one individual with more branches of the cardiovascular system. In simulation all the arterial walls should be made elastic and mobile for more realistic blood transition simulation. If the blood transition path is closer to realistic other tissue layers can be placed between the electrodes on the surface of the skin and arteries, and then proceeded with analysis and further study of complex human cardiovascular system.

References

[1] K. A. Zimmermann, “Circulatory System: Facts, Function & Diseases,” *LIVESCIENCE*, 2018. [Online]. Available: https://www.livescience.com/22486-circulatory-system.html. [Accessed: 01-Apr-2019].

[2] J. Rehman, “Advantages and disadvantages of simulation,” *IT Release*, 2018. [Online]. Available: http://www.itrelease.com/2018/09/advantages-and-disadvantages-of-simulation/. [Accessed: 03-Apr-2019].

[3] “Computational Modeling,” *NIBIB*, 2016. [Online]. Available: https://www.nibib.nih.gov/sites/default/files/Computational_Modeling_Fact_Sheet_ENGLISH_v4_508_0.pdf. [Accessed: 03-Apr-2019].

[4] R. Crachmaliuc, “75 Years of the Finite Element Method (FEM),” *SIMSCALE*, 2019. [Online]. Available: https://www.simscale.com/blog/2015/11/75-years-of-the-finite-element-method-fem/. [Accessed: 03-Apr-2019].

[5] A. Harish, “Finite Element Method – What Is It? FEM and FEA Explained,” *SIMSCALE*, 2019. [Online]. Available: https://www.simscale.com/blog/2016/10/what-is-finite-element-method/. [Accessed: 04-Apr-2019].

[6] L. Caudill and A. Barnhorn, “60 Years of CAD Infographic: The History of CAD since 1957,” *CADENAS*, 2018. [Online]. Available: https://partsolutions.com/60-years-of-cad-infographic-the-history-of-cad-since-1957/. [Accessed: 04-Apr-2019].

[7] “Cardiovascular disease,” *WHO*, 2016. [Online]. Available: https://www.who.int/cardiovascular_diseases/en/. [Accessed: 05-Apr-2019].

[8] “Heart Disease: Types,” *Harvard University*, 2018. [Online]. Available: https://www.hsph.harvard.edu/nutritionsource/disease-prevention/cardiovascular-disease/cvd-types/. [Accessed: 05-Apr-2019].

[9] A. Avolio, “Central Aortic Blood Pressure and Management of Hypertension,” *AHA Journals*, 2013. .

[10] C. M. McEniery, J. R. Cockcroft, M. J. Roman, S. S. Franklin, and I. B. Wilkinson, “Central blood pressure: current evidence and clinical importance,” *Ozford Journals*, 2014. .

[11] A. L. Pauca, S. L. Wallenhaupt, N. D. Kon, and W. Y. Tucker, “Does Radial Artery Pressure Accurately Reflect Aortic Pressure?,” *ScienceDirect*, 1992. .

[12] M. F. O'Rourke and A. Adij, "Noninvasive Studies of Central Aortic Pressure," *SpringerLink*, 2011. .

[13] K. Takazawa, H. Kobayashi, N. Shindo, N. Tanaka, and A. Yamashima, "Relationship between radial and central arterial pulse wave and evaluation of central aortic pressure using the radial arterial pulse wave," *NATURE*, 2007. .

[14] A. Krotov, "Simulation of electric impedance measurement on a 3D human arm model," Tallinn University of Technology, 2017.

[15] P. Vasava, P. Jalali, M. Dabagh, and P. J. Kolari, "Finite Element Modelling of Pulsatile Blood Flow in Idealized Model of Human Aortic Arch: Study of Hypotension and Hypertension," *Lappeenranta University of Technology*, 2011. .

[16] P. Vasava, P. Jalali, M. Dabagh, and P. J. Kolari, "Finite Element Modelling of Pulsatile Blood Flow in Idealized Model of Human Aortic Arch: Study of Hypotension and Hypertension," *Lappeenranta University of Technology*, 2012. .

[17] A. Nardi, M. Brand, M. Halak, M. Ratan, D. Silberberg, and I. Avrahami, "Hemodynamical Aspects of Endovascular Repair for Aortic Arch Aneurisms," *IFMBE*, 2013. .

[18] D. Afkari, "Pulsatile blood flow interactionwith arterial walls of aorta:autoregulation and impedancepressure boundary conditionand its biomedical applications," 2015.

[19] T. Barclay, "Cardiovascular System," *innerbody*, 2018. [Online]. Available: https://www.innerbody.com/image/cardov.html. [Accessed: 08-Apr-2019].

[20] "How does the blood circulatory system work?," *IQWiG*, 2010. [Online]. Available: https://www.ncbi.nlm.nih.gov/books/NBK279250/. [Accessed: 08-Apr-2019].

[21] A. Cattamanchi, A. Carter, A. Biggers, A. Gonzalez, and A. M. Griff, "Circulatory," *Healthline*, 2015. [Online]. Available: https://www.healthline.com/human-body-maps/circulatory-system#1. [Accessed: 08-Apr-2019].

[22] O. Jones, "Arterial Supply to the Upper Limb," *TeachMeAnatomy*, 2019. [Online]. Available: https://teachmeanatomy.info/upper-limb/vessels/arteries/. [Accessed: 09-Apr-2019].

[23] S. Grimnes and O. G. Martinsen, *Bioimpedance and bioelectricity basics*, Third. UK, USA: Elseiver Ltd, 2015.

[24] C. Cornelius, J. Sorber, R. A. Peterson, J. Skinner, R. J. Halter, and D. Kotz, "Who Wears Me? Bioimpedance as a Passive Biometric," *HealthSec*, 2012. [Online]. Available: https://www.semanticscholar.org/paper/Who-Wears-Me-Bioimpedance-as-a-Passive-Biometric-Cornelius-Sorber/0fae1ea8dde7503b232b71a85d4d88a18c032bf5. [Accessed: 12-Apr-2019].

[25] D. S. Holder, *Electrical Impedance Tomography: Methods, History and Applications*. UK: IOP Publishing Ltd, 2005.

[26] U. G. Kyle *et al.*, "Bioelectrical impedance analysis—part I: review of principles and methods," *ESPEN*, 2004. .

[27] K. R. Visser, "Electric properties of blood and impedance cardiography," *University of Groningen*, 1992. [Online]. Available: https://www.rug.nl/research/portal/files/14483850/steen0001.PDF. [Accessed: 15-Apr-2019].

[28] D.-H. Nam, W.-B. Lee, Y.-S. Hong, and S.-S. Lee, "Measurement of Spatial Pulse Wave Velocity by Using a Clip-Type Pulsimeter Equipped with a Hall Sensor and Photoplethysmography," *MDPI*, 2013. .

[29] R. L. Gaw, "The Effect of Red Blood Cell Orientation onthe Electrical Impedance of Pulsatile Bloodwith Implications for Impedance Cardiography," *Queensland University of Technology*, 2010. [Online]. Available: https://core.ac.uk/download/pdf/10902128.pdf. [Accessed: 12-Apr-2019].

[30] M. Hoffman, "Picture of Blood," *WebMD*, 2019. [Online]. Available: https://www.webmd.com/heart/anatomy-picture-of-blood#1. [Accessed: 04-Apr-2019].

[31] J. Lucas, "What Is Fluid Dynamics?," *LIVESCIENCE*, 2014. [Online]. Available: https://www.livescience.com/47446-fluid-dynamics.html. [Accessed: 11-Apr-2019].

[32] H. E. A. Baieth, "Physical Parameters of Blood as a Non - Newtonian Fluid," *IJBS*, 2008. [Online]. Available: https://www.ncbi.nlm.nih.gov/pmc/articles/PMC3614720/. [Accessed: 08-Apr-2019].

[33] S. Canic, "FLUID-STRUCTURE INTERACTIONIN BLOOD FLOW," *MSRI*, 2006. [Online]. Available: https://pdfs.semanticscholar.org/99b8/b303b76e20dafed23edcb690d833bf37ffd5.pdf. [Accessed: 01-May-2019].

[34] M. Fowler, "Viscosity I: Liquid Viscosity," 2019. [Online]. Available: http://galileo.phys.virginia.edu/classes/152.mf1i.spring02/Viscosity.htm. [Accessed: 04-Apr-2019].

[35] A. Paar, "Viscosity measurement of whole blood," *Anton Paar Ltd*, 2016. [Online]. Available: https://www.muser-my.com/wp-content/uploads/2018/11/C72IA025EN-B_Viscosity_of_Whole_Blood.pdf. [Accessed: 15-Apr-2019].

[36] S. H. Wang, "A linear relation between the compressibility and density of blood," *ASA*, 2000. .

[37] J. D. Cutnell and K. W. Johnson, *Physics*, Fourth. Wiley, 1997.

[38] M. Syed, “HEMODYNAMICS – BLOOD FLOW VELOCITY,” *drbeen*, 2018. [Online]. Available: https://www.drbeen.com/blog/physiolgy-lecture-3-study-notes-hemodynamics-blood-flow-velocity/. [Accessed: 13-Apr-2019].

[39] R. Kurtus, “Fluid Pressure,” 2017. [Online]. Available: https://www.school-for-champions.com/science/fluid_pressure.htm#.XM60T9hS-Cg. [Accessed: 22-Apr-2019].

[40] T. Newman, “The heart: All you need to know,” *MedicalNewsToday*, 2018. [Online]. Available: https://www.medicalnewstoday.com/articles/320565.php. [Accessed: 14-Apr-2019].

[41] R. E. Klabunde, “Bernoulli’s Principle and Energetics of Flowing Blood,” 2019. [Online]. Available: https://www.cvphysiology.com/Hemodynamics/H012. [Accessed: 09-Apr-2019].

[42] H. Xiao, M. Butlin, I. Tan, A. Qasem, and A. P. Avolio, “Estimation of Pulse Transit Time From Radial Pressure Waveform Alone by Artificial Neural Network,” *IEEE*, 2017. .

[43] J. T. Ottesen, M. Olufsen, and J. K. Larsen, “Applied Mathematical Models in Human Physiology,” *SIAM*, 2004. .

[44] B. Koeppen and B. Stanton, “Berne & Levy Physiology,” *Elsevier*, 2008. [Online]. Available: http://users.atw.hu/blp6/BLP6/HTML/C0159780323045827.htm. [Accessed: 15-Apr-2019].

[45] V. P. S. Fazan, C. T. Borges, J. H. de Silva, A. G. Caetano, and O. A. R. Filho, “Superficial palmar arch: an arterial diameter study,” *Journal of Anatomy*, 2004. .

[46] A. M. Manole, D. M. Iliescu, A. Rusali, and P. Bordei, “Morphometry of the aortic arch and its branches,” *VERSITA*, 2013. .

[47] J.-P. Barral and A. Croibier, “The subclavian arteries,” *Visceral Vascular Manipulations*, 2011. .

[48] R. Tayal *et al.*, “CT Angiography Analysis of Axillary Artery Diameter versus Common Femoral Artery Diameter: Implications for Axillary Approach for Transcatheter Aortic Valve Replacement in Patients with Hostile Aortoiliac Segment and Advanced Lung Disease,” *International journal of vascular medicine*, 2016. .

[49] S. Majumdar, S. Bhattacharya, A. Chetterjee, H. Dasgupta, and K. Bhattacharya, “A Study on Axillary Artery and its Branching Pattern among the Population of West Bengal, India,” *IJAE*, 2013. .

[50] Y. Tomiyama *et al.*, “Accurate quantitative measurements of brachial artery cross-sectional vascular area and vascular volume elastic modulus using automated oscillometric measurements: comparison with brachial artery ultrasound,” *Hypertension*

Research, 2015. .

[51] V. V. G. Patnaik, G. Kalsey, and K. S. Rajan, "Branching Pattern of Brachial Artery-A Morphological Study," *Patiala Medical College*, 2002. [Online]. Available: http://medind.nic.in/jae/t02/i2/jaet02i2p176.pdf. [Accessed: 10-Apr-2019].

[52] S. Beniwal, K. Bhargava, and S. K. Kausik, "Size of distal radial and distal ulnar arteries in adults of southern Rajasthan and their implications for percutaneous coronary interventions," *Elsevier*, 2014. .

[53] A. Y. Nasr, "The radial artery and its variations:anatomical study and clinical implications," *VIA Mesica*, 2012. [Online]. Available: https://pdfs.semanticscholar.org/b665/d0b942cc9263033c1bc31dc1e12a30c533ef.pdf. [Accessed: 10-Apr-2019].

[54] D. Andreuccetti, R. Fossi, and C. Petrucci, "Dielectric Properties of Body Tissues," *IFAC*, 2015. [Online]. Available: http://niremf.ifac.cnr.it/tissprop/htmlclie/htmlclie.php. [Accessed: 01-May-2019].

[55] K. Takashima, T. Kitou, K. Mori, and K. Ikeuchi, "Simulation and experimental observation of contact conditions between stents and artery models," *PubMed*, 2007. .

[56] J. J. R. Fojas and R. L. De Leon, "Carotid Artery Modeling Using the Navier-Stokes Equations for an Incompressible, Newtonian and Axisymmetric Flow," *APCBEE*, 2013. .

[57] COSMOL, "COMSOL Multiphysics 5.2 manual," 2019.

[58] "What is the Reynolds Number?," *SimWiki*, 2017. [Online]. Available: https://www.simscale.com/docs/content/simwiki/numerics/what-is-the-reynolds-number.html. [Accessed: 10-Apr-2019].

[59] J. Soulis, G. Giannoglou, M. Dimitrakopoulou, V. Papaioannou, S. Logothetides, and D. Mikhailidis, "Influence of Oscillating Flow on LDL Transport and Wall Shear Stress in the Normal Aortic Arch," *Bentham open*, 2009. [Online]. Available: https://www.ncbi.nlm.nih.gov/pmc/articles/PMC2761669/. [Accessed: 13-Apr-2019].

[60] A. J. M. Lewis and D. Kotecha, "CAROTID VERSUS RADIAL PULSE WAVE ANALYSIS," *BMJ*, 2013. .

Appendix 1 – PC specifications

PC 1 (with COMSOL Multiphysics version 5.2)

Operating system	Windows 7 Ultimate 64-bit
CPU	Intel Core i7 4702MQ @ 2.20GHz
RAM	8GB DDR3 @ 798MHz
Graphics card	2047MB NVIDIA GeForce GT 820M